# Multiresolution LBP for lace images classification

V. Truong Hoang
HCMC Open University
Ho Chi Minh City, Vietnam
e-mail: vinh.th@ou.edu.vn

## Abstract

*The lace images are particularly difficult to be analyzed in digital form using classical image processing and machine vision techniques. The major reasons of this difficulty emerge from their fine complex structure and pattern. In this work, the major approaches implied for the evaluations of lace images are Image Histogram and Local Binary Patterns (LBP). Two variants of LBP are mainly evaluated. The accuracy obtained of each descriptor via the k-NN classifier with different distances. Experimental results indicate that the basic LBP generates the best performance 97% under neutral variation.*

**Keywords**: lace image, texture analysis, classification, LBP, k-NN classifier.

## 1 Introduction

Indexing and searching images in large databases are currently considered two advanced search fields [1, 6]. In particular, the indexing step is more decisive in which the image is analyzed in order to extract the features (such as the distribution, vector attributes, etc.) characterizing the images. The discrimination of these features is related to the content of the image. Several indexing applications are developed on the image: textures [2], faces [3]. However, there is no lace image indexing application since lace is considered a national cultural heritage in some regions. This may be due to the complex nature of the lace. Indeed, lace is generally made by different parts with different textures: the background, the basic pattern, the decoration, etc. Also, the diversity of the lace samples and the acquisition conditions including different rotations and different scale factors can also make their treatments difficult.

In the literature, several works focus on the lace images related to the fabric detection (hole, distortion, tear) during the manufacture of lace [3, 4] and generally during the manufacture of textiles [5, 6, 7]. These approaches aim to produce fast and reliable algorithms for the measurement, analysis and real-time control of textile production processes. Nevertheless, several works are interested in the post-production phase such as the detection of garment defects [8] and the recognition of patterns in clothing [9].

In this work, we present a study of lace images using multiresolution local binary patterns (MS-LBP) by the presence of several rotation and scaling factors. The rest of this article is organized as follows. Section 2 introduces MS-LBP. Section 3 presents the classification method. Sections 4 and 5 describe the experimental protocol and the experimental results, respectively. Finally, section 6 gives the conclusion and perspectives.

## 2 The Multiresolution Local Binary Pattern

The Local Binary Pattern (LBP) operator was firstly proposed by Ojala [9]. The idea of this descriptor is to assign each pixel a code depending on the gray levels of its neighborhood. The gray level of the central pixel $g_c$ is compared to its neighbors according to the following formula:

$$\mathrm{LBP}(x_c, y_c) = \sum_{i=0}^{P} s(g_i - g_c) \times 2^i \quad (1)$$

Where $s(.)$ is a threshold function and is defined as follows:

$$s(g_i - g_c) = \begin{cases} 1 & if \quad g_i - g_c \geq 0 \\ 0 & otherwise \end{cases} \quad (2)$$

With $P$ is the number of neighboring pixels. In our work, we consider a neighborhood of 3 × 3 which allows to have 8 neighbors. We thus obtain, as for a grayscale image, a matrix containing LBP values for each pixel between 0 and 255. A histogram is calculated based on these values to form the LBP descriptor of an image. Subsequently, this descriptor has been extended using neighborhoods in different size [11, 12, 15]. In this case, a circle of radius $R$ around the central pixel is considered. The values of the $P$ points sampled at the edge of this circle are taken and compared with the value of the central pixel. To obtain the values of the $P$ points sampled in the neighborhood for any radius $R$. The notation ($P$, $R$) is adopted to define the neighborhood of $P$ points of radius $R$ of a pixel. In our experiments, $R$ belongs to the interval I = [1,...,10] and the neighborhood $P$ varies among the values {4, 8, 12, 16}. In order to reduce the size of the LBP descriptors, the bits transition of LBP code is selected to form LBP Uniform [10]. On the other hand, to take account of information rotation, a specific coding is adopted to form the invariant LBP for rotation [10]. In this case, uniform LBP invariant to rotation transform [10] is created to reduce the size of rotation-invariant LBP.

## 3 k-NN classifier

After a feature extraction step, we proceed to the classification of the samples based on the different descriptors. In this work, the k nearest neighbor method (k-NN) has been applied. In this case, we have a learning database consisting of N "sample-class" pairs. To estimate the output associated with a new input $\boldsymbol{x}$, the k-NN method consists of considering the k training samples whose input is closest to the new input $\boldsymbol{x}$, according to a distance to be defined. For example, in our classification problem, we will retain the class most represented among the k outputs associated with the k entries closest to the new entry $\boldsymbol{x}$. The considered distances [12] are the histogram intersection (Eq.3), the likelihood log (Eq.4) and the Chi-square distance (Eq.5).

$$d(x,y) = \sum_{b=1}^{B} min(x_b y_b) \quad (3)$$

$$d(x,y) = -\sum_{b=1}^{B} x_b log(y_b) \quad (4)$$

$$d(x,y) = \sum_{b=1}^{B} \frac{(x_b - y_b)^2}{(x_b + y_b)} \quad (5)$$

where, $x \in R^{1x\,B}$ and $y \in R^{1x\,B}$ are two vectors extracted from the lace images.

## 4 The experimental protocol

The experimental protocol makes it possible to present the various experimentation scenarios as well as the decomposition of the image database.

### 4.1 Construction the image database

The base of lace images consists of 41 images of lace bottoms (see Figure 1). The background images of laces called lace samples were extracted from the registers kept in the International Center of Lace and Fashion. The original registers in paper form were scanned in color version. We extract from each image of lace thumbnails of fixed size (150 x 150 pixels).

### 4.2 Experimental scenarios

In our experiments, the initial image database consists of 592 images of lace obtained from the 41 lace bottoms. Each lace background has generated 12 lace stock images. This base has been divided into two subsets: learning base and testing basis (decomposition 1). The testing database was then enriched by new test images corresponding to the initial test images to which we applied transformations such as: rotations of 90°, 180° and 270° (decomposition 2), changes of scale of factors 0.5 and 2

(decomposition 3) and the two transformations combined (decomposition 4). Table 1 shows all the decompositions mentioned.

At the level of the k-NN classification algorithm, the number 'k' of nearest neighbors is fixed at 1, the distance 'D' is defined by the three distances (see section 4). The accuracy rate, which represents the number of correctly classified samples based on the total number of samples, is adopted as an evaluation criterion.

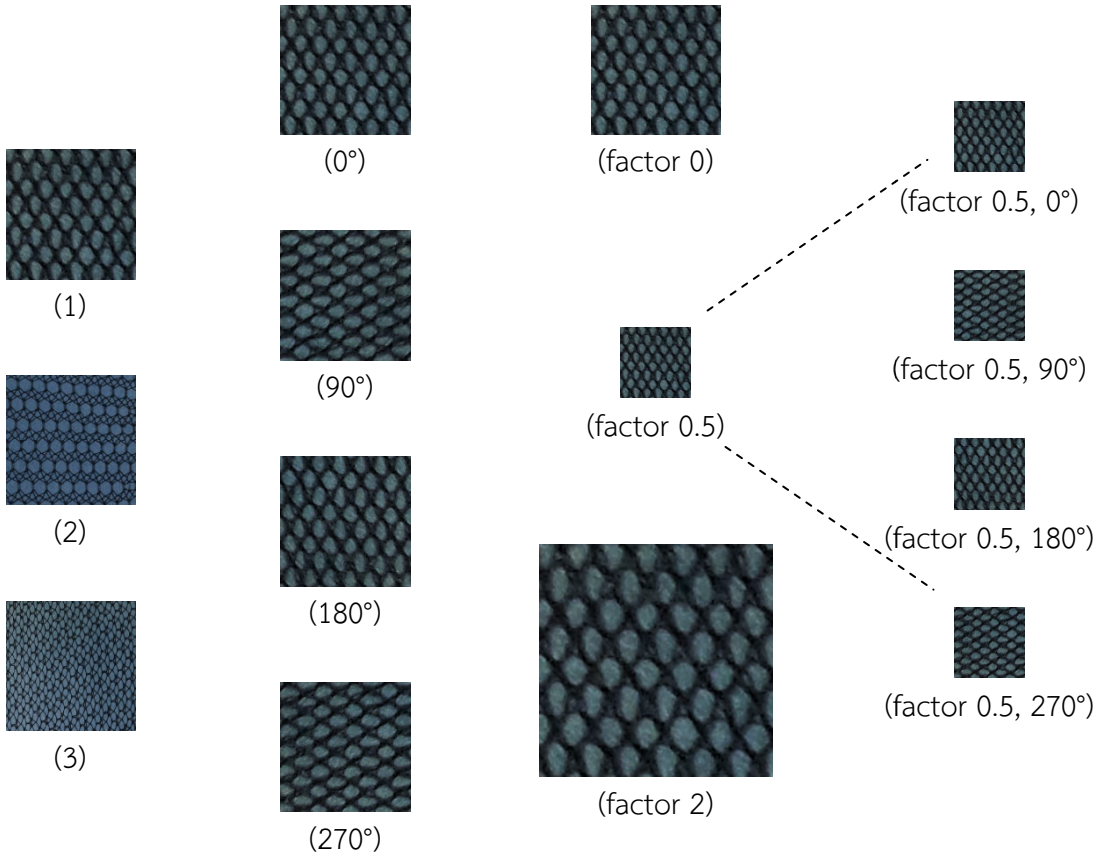


| (a) 3 different lace images with basic pattern | (b) Application of rotation transformation on the basic pattern (1) | (c) Application of scale change transformation on the basic pattern (1) | (c) Application of rotation transformation and scale change on the basic pattern (1) |
|---|---|---|---|

**Figure 1.** Example of lace background images with different transformations of rotation and change of scale

**Table 1.** The different decompositions of the image database

| Number of Decomposition | Size of the learning set | Size of the testing set |
|---|---|---|
| 1 | 246 × (6 × 41) | 246 × (6 × 41) |
| 2 | 246 × (6 × 41) | 984 × (4 × 6× 41) |
| 3 | 246 × (6 × 41) | 738 × (3 × 6 × 41) |
| 4 | 246 × (6 × 41) | 2952 × (12 × 6 × 41) |

## 5 Experimental results

In each scenario and for each LBP variant, we applied cross-validation with 20 experiments. For each experiment, we randomly selected 6 learning images and 6 test images for each lace background image. The average accuracy is adopted to show the different performances.

### 5.1 Scenario 1: Without transformation

In the first scenario, the images of the decomposition 1 made it possible to test all the variants LBP. Figure 2 presents the classification rates for the different LBP variants as a function of the value of $R$. We have chosen for each radius $R$ the maximum of the classification rate corresponding to a neighborhood $P$ selected from the values {4, 8, 12, 16}.

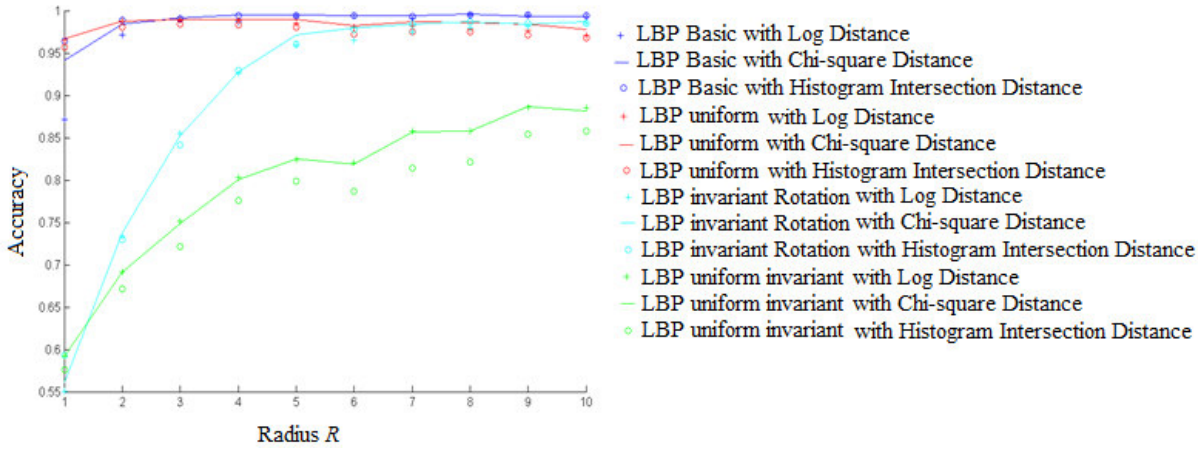


Figure 2. Classification rate as a function of the radius $R$ of the different LBP variants using the Log-likelihood, Chi-square and Histogram Intersection distances

Based on the results, the basic LBP generated the best performance with all $R$ values except $R$ = {1, 2}. Specifically, the best 99.67% classification rate was generated by LBP-Basic for $R$ = 8, $P$ = 12, with Chi-square distance. We detail the performance of LBP Basic with the different neighborhoods in Figure 3. From this Figure, we can observe that by

increasing the radius $R$ and whatever the neighborhood $P$, the classification rate also increases. This result is explained by the nature of the lace which has a texture discerned with large values of radius $R$. According to Figure. 3, the value of the neighborhood $P$ = 4 did not favor a description adequate contrary to the values $P$ = {8, 12, 16}. We note an average classification rate of 88.18% for $P$ = 4 which is significantly lower than the 98.50%, 98.73%, 97.47% rates generated respectively by $P$ = 8, $P$ = 12, $P$ = 16.

### 5.2 Scenario 2: Rotation Transformation

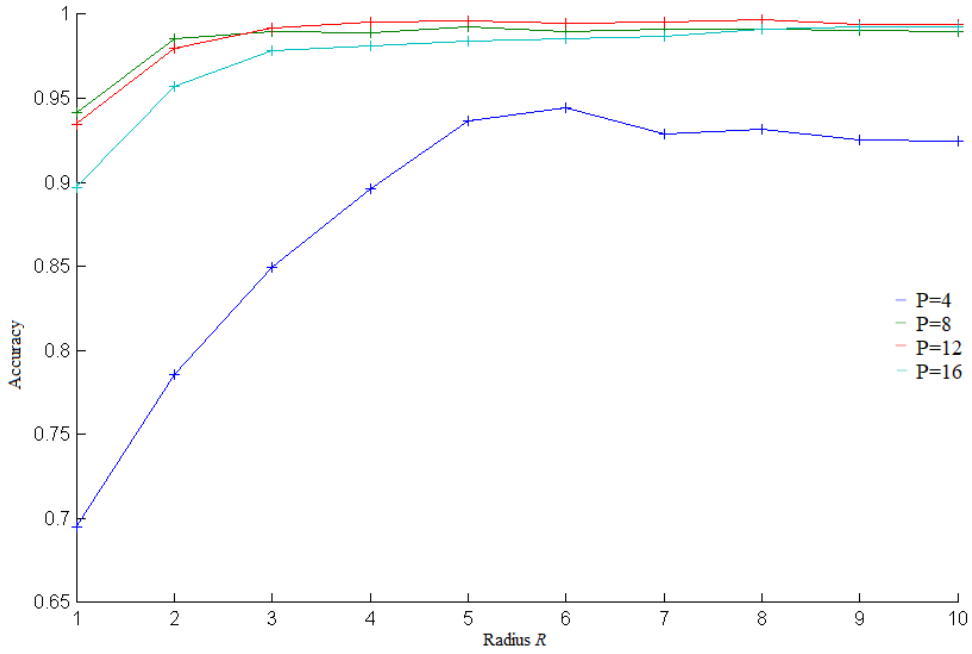


Figure 3. Classification according to the $R$ (radius) and $P$ (neighborhood) parameters of the basic LBP using the Chi-square distance

In this scenario, the decomposition 2 images were used to test all LBP variants. Figure 4 presents the classification rate for the LBP variants as a function of the $R$ parameter. For each radius, we have chosen the maximum of the classification rate corresponding to a neighborhood $P$ selected from the values {4, 8, 12, 16}. Based on the results, the rotation-invariant LBP generated the best performance with all $R$ values except for $R$ = {1}. Specifically, the best classification rate of the order of 98.80% was generated by LBP Invariant at rotation for $R$ = 8, $P$ = 12, with the distance Chi-square.

We detail the performance of the LBP Invariant to the rotation with the different neighborhoods in Figure 4. From this figure, the comparison between LBP Basic and LBP

Uniform, LBP Invariant at rotation allowed to reach the best performance. This is explained by the choice of the coding adopted at the rotation-invariant LBP which considers the presence of rotation transformation. By increasing the radius $R$ and whatever the neighborhood size, the classification rate increases.

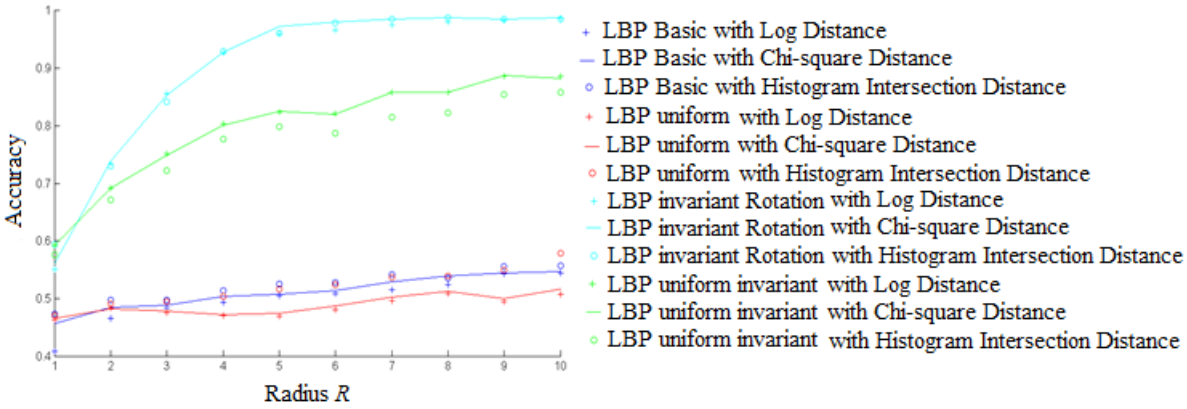


**Figure 4.** Classification rate as a function of the radius $R$ of the different LBP variants using the Log-likelihood, Chi-square and Histogram Intersection distances

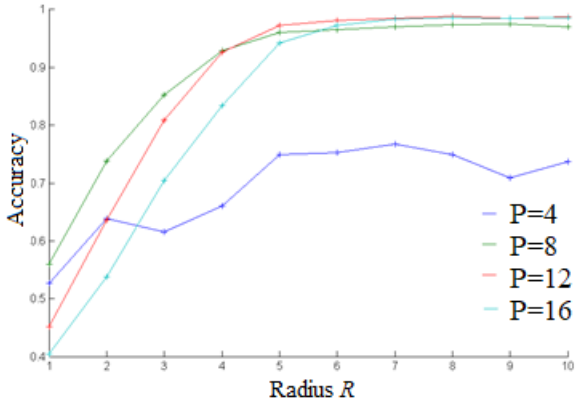


**Figure 5.** Classification rate according to $R$ (radius) and $P$ (neighborhood) parameters of LBP Invariant to rotation using Chi-square distance

From Figure 5, we detect the same performance as Scenario 1 in the case where the neighborhood $P$ = 4 contrary to the values $P$ = {8, 12, 16}. We note an average classification rate of 69.08% which is significantly lower than the 88.96%, 87.21%, 83.36% rates generated respectively by $P$ = 8, $P$ = 12, $P$ = 16. It is obvious that by increasing the radius $R$, a neighborhood $P$ = 4 is insufficient to code the neighboring pixels.

### 5.3 Scenario 3: Scaling Transformation

Applying scaling factor transformation on decomposition test images 3, we evluated all LBP variants. Figure 6 shows the classification rate for the LBP variants as a function of the $R$ parameter. We have chosen for each radius the maximum of the classification rate corresponding to a neighborhood $P$ selected from the values {4, 8, 12, 16}. According to the results, no variant LBP has exceeded 60% of classification rate with all the radius. This weak discrimination is explained by the influence of the change of scale on the coding adopted at the level of the LBP.

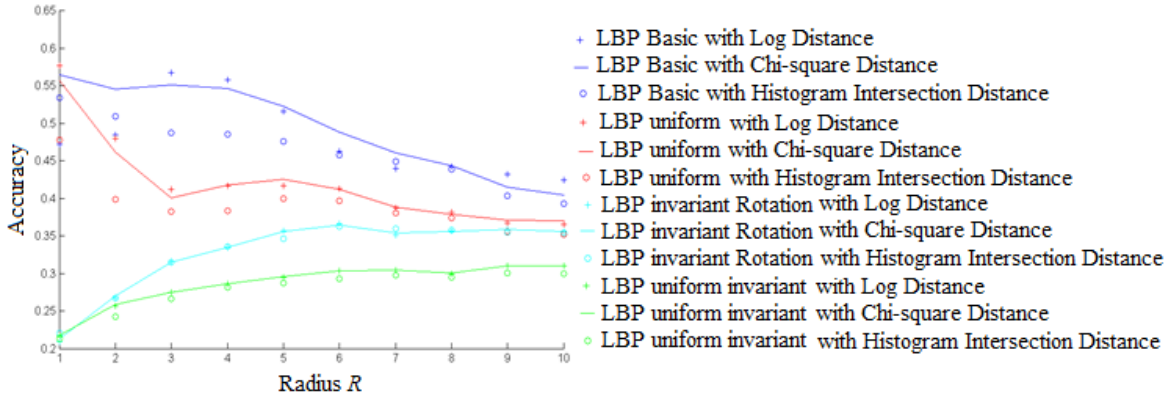


**Figure 6.** Classification rate as a function of the radius $R$ of the different LBP variants using the Log-likelihood, Chi-square and Histogram Intersection distances

By increasing the radius $R$, all the neighborhoods exhibit the same performance with a slight improvement in terms of classification. for the neighborhood $P$ = 16 (see in Figure 7.).

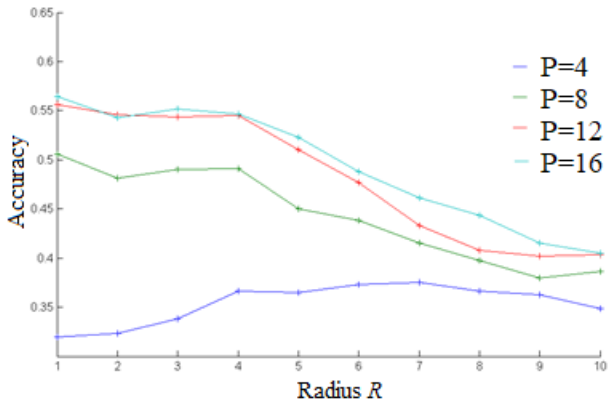


**Figure 7.** Classification rate according to the $R$ (radius) and $P$ (neighborhood) parameters of the Basic LBP using Chi-square distance

### 5.4 Scenario 4: Combined Rotation and Scaling Transformation

In this last scenario, the images of the decomposition 4 made it possible to test all the variants LBP. Figure 8 presents the classification rate for the LBP variants as a function of the $R$ pa-rameter. We have chosen for each radius the maximum of the classification rate corresponding to a neighborhood $P$ selected from the values {4, 8, 12, 16}. According to the results, the rotational invariant LBP generated the best performances with all $R$ values except for $R$ = {1, 2}. However, the classification rate did not exceed 40% of the classification rate. This low discrimination is due to the influence of rotation transformation and scaling on the coding adopted at the LBP level.

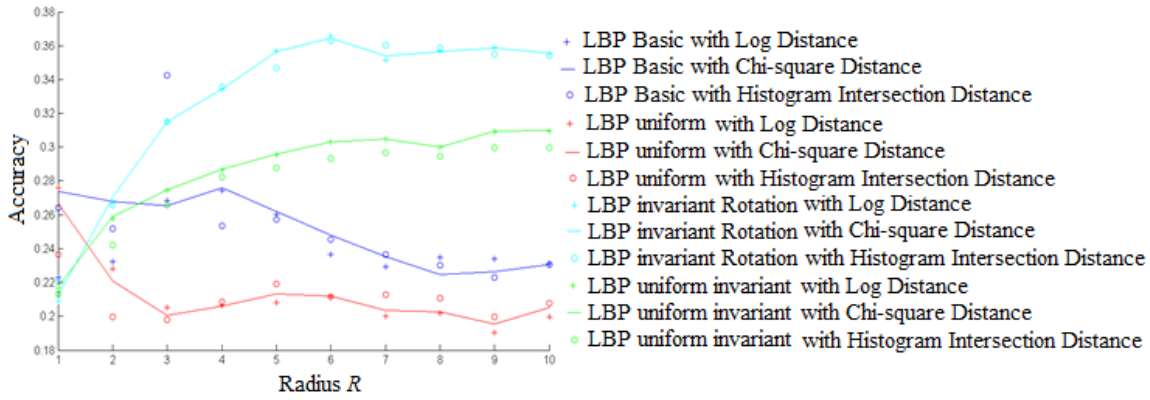


**Figure 8.** Classification rate according to the radius $R$ of the different LBP variants using the log-likelihood, chi-square and histogram intersection

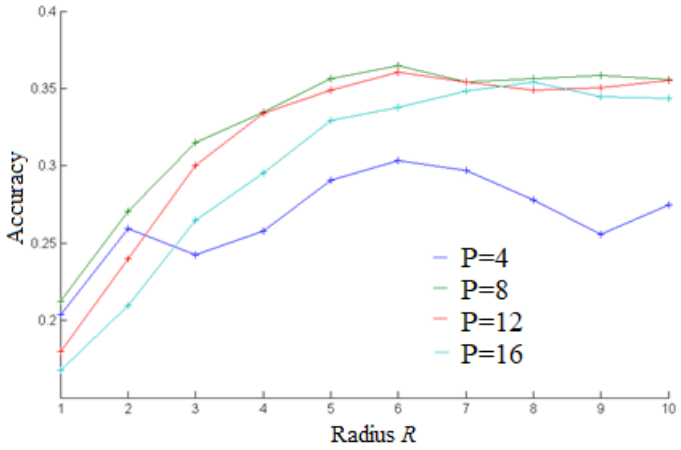


**Figure 9.** Classification rate according to $R$ (radius) and $P$ (neighborhood) parameters of LBP Invariant to rotation using Chi-square distance

We detail the performance of the LBP Invariant to the rotation, which generated the best performances, with the different neighborhoods in Figure 9. It is clear that by increasing the radius $\boldsymbol{R}$, the neighborhoods $\boldsymbol{P}$ = {8, 12, 16} give the same performance.

## 6 Conclusion

In this article, we analyzed the performance of multiresolution local binary patterns extracted from lace images in the presence of several rotation and scaling factors. The experimental results show that the multiresolution LBP give a better classification by choosing large values of the radius $\boldsymbol{R}$ whatever the value of the neighborhood of the pixels $\boldsymbol{P}$. In the presence of the transformation of rotation, the LBP Invariant to the rotation presents a robustness compared to other variants of LBP. In the case of scaling presence, all performance dropped significantly for all LBP variants. As perspectives, we will focus on proposing the contribution of fusion for all LBP variants with respect to different transformations.

## References

[1] L. Piras and G. Giacinto, “Information fusion in content-based image retrieval: A comprehensive overview,” Information Fusion, vol. 37, pp. 50–60, Sep. 2017.

[2] T. Ojala, T. Mäenpää, M. Pietikäinen, J. Viertola, J. Kyllönen, and S. Huovinen, "Outex new framework for empirical evaluation of texture analysis algorithms," In Proceedings of the 16th International Conference on Pattern Recognition, vol. 1, pp. 701–706, 2002.

[3] K. I. Chang, K. W. Bowyer, and P. J. Flynn, "An Evaluation of multimodal 2D+3D Face Biometrics," IEEE Trans. Pattern Anal. Mach. Intell. 27(4), pp. 619-624, 2005.

[4] C. Sanby, L. Norton-Wayne and R. Harwood, "The automated inspection of lace using machine vision," Mechatronics Vol. 5, No. 2/3, pp. 215-231, 1995.

[5] L. Norton-Wayne, "Inspection of lace using machine vision," Comput. Graph. Forum 10, pp. 113-119, 1991.

[6] C. Singh, E. Walia, and K. P. Kaur, “Color texture description with novel local binary patterns for effective image retrieval,” Pattern Recognition, vol. 76, pp. 50–68, Apr. 2018.

[7] B. Olanviriyakij, S. Jumreornvong, and P. Kumhom, “A detection of tears in laces using image processing,” in Knowledge and Smart Technology (KST), 2015 7th International Conference on, 2015, pp. 195–198.

[8] M. Tabassiana, R. Ghaderi , R. Ebrahimpour, " Knitted fabric defect classification for uncertain labels based on Dempster-Shafer theory of evidence," Expert Systems with applications, 38 (5), pp. 5259–5267, 2011.

[9] C. W. M. Yuen, W. K. Wong, S.Q. Qian, L.K. Chan, E. H. K. Fung, "A hybrid model using genetic algorithm and neural network for classifying garment defects," Expert Systems with ap-plications, vol. 36 (2), Part 1, pp. 2037–2047, 2009.

[10] M. C. Y. Cheong, and K.-S. Loke, "Textile recognition using tchebichef moments of co-occurrence matrices," ICIC 1, vol. 5226 of Lecture Notes in Computer Science, pp. 1017-1024. Springer, 2008.

[11] T. Ojala, M. Pietikainen., and D. Harwood, "A comparative study of texture measures with classification based on feature distributions," Pattern Recognition 29 (1), pp. 51-59, 1996.

[12] T. Ojala, M. Pietikainen and T. Maenpaa, "Multiresolution gray-scale and rotation invariant texture classification with local binary patterns," IEEE Transactions on Pattern Analysis and Machine Intelligence, vol. 24 (7), pp. 971-987, 2002.

[13] W. Ben Soltana, D. Huang, M. Ardabilian, L. Chen, C. Ben Amar, “A mixture of gated experts optimized using Simulated Annealing for 3D Face Recognition,” International Conference on Image Processing (ICIP), Brussels, Septembre 11 -14, 2011.

[14] T. Ahonen, A. Hadid, M. Pietikäinen, Face recognition with local binary pattern. Computer vision, ECCV, pp. 469-481, 2004.

[15] L. Liu, P. Fieguth, Y. Guo, X. Wang, and M. Pietikäinen, “Local binary features for texture classification: Taxonomy and experimental study,” Pattern Recognition, vol. 62, pp. 135–160, Feb. 2017.

[16] J. Jinga, H. Zhanga, P. Lia, "Improved Gabor filters for textile defect detection," Procedia Engineering, vol. 15, pp. 5010–5014, 2011.